

Parton rescattering and screening in Au+Au collisions at RHIC

S. A. Bass,^{1,2} B. Müller,¹ and D. K. Srivastava^{1,*}

¹*Department of Physics, Duke University, Durham, NC 27708-0305, USA*

²*RIKEN BNL Research Center, Brookhaven National Laboratory, Upton, NY 11973, USA*

We study the microscopic dynamics of quarks and gluons in relativistic heavy ion collisions in the framework of the Parton Cascade Model. We use lowest order perturbative QCD cross sections with fixed lower momentum cutoff p_T^{min} . We calculate the time-evolution of the Debye-screening mass μ_D for Au+Au collisions at $\sqrt{s} = 200$ GeV per nucleon pair. The screening mass is used to determine a lower limit for the allowed range of p_T^{min} . We also determine the energy density reached through hard and semi-hard processes at RHIC, obtain a lower bound for the rapidity density of charged hadrons produced by semihard interactions, and analyze the extent of perturbative rescattering among partons.

The first experimental results from the Relativistic Heavy Ion Collider (RHIC) have generated a vast amount of interesting data [1, 2]. A variety of theoretical models has been invoked to describe the observed phenomena, e.g., fluid dynamical models, perturbative QCD scattering models, as well as models based on parton saturation and statistical approaches. Although these models, which all contain adjustable parameters, have been fairly successful within their respective regimes of anticipated applicability, they all have certain limitations. For example, fluid dynamics cannot describe transport phenomena occurring prior to local equilibration of the produced matter, and it must fail above a certain, though unknown, value of p_T . Perturbative parton scattering models cannot describe the physics of equilibration and the formation of collective flow. Initial state parton saturation models do not include the final state interaction among partons, which leads to equilibration.

The parton cascade model (PCM) was proposed, about a decade ago, with the aim to provide a unified framework for the description of phenomena involving high and intermediate values of p_T [3]. It is based on the premise that the microscopic dynamics during the early stages of a high-energy nuclear collision can be described as a cascade of two-body interactions among perturbative quarks and gluons, with certain modifications caused by the presence of a hot and dense medium. Because of its perturbative nature, the PCM cannot describe the hadronization stage, unless additional phenomenological models are introduced.

Since the original formulation and implementation of the PCM by Geiger (VNI) [4], significant new insights into the dynamics of dense systems of partons have been gained. First and foremost among these is the applicability of semiclassical methods for the description of the partonic structure in the initial state and the earliest phase of its evolution [5]. Another relevant development is the recognition of the importance of radiative processes for the attainment of local thermal equilibrium in the rapidly

expanding matter. Radiative processes were already included in the original PCM in the leading-logarithmic approximation (LLA). The concept of initial-state saturation of the parton distribution, however, provides a novel feature which can be utilized to address the infrared divergences of the perturbative PCM.

In this letter we focus on the early, pre-thermal reaction phase of a heavy-ion reaction and address the following questions:

- What limits on the cut-off p_T^{min} , required by the infra-red divergence of the pQCD cross section, are imposed by the internal consistency of the model and by existing data on particle distributions?
- What energy-density and multiplicity is reached through hard and semi-hard processes (alone) at RHIC within these limits?
- Do partons undergo multiple perturbative binary collisions? Are these sufficient to produce (measurable) collective effects?

We will here restrict our discussion of the results from the Parton Cascade Model implementation (VNI/BMS, an improved and corrected version of the VNI implementation [4]) to binary processes in leading order pQCD – a more detailed calculation involving NLO corrections such as radiative processes will be presented in a forthcoming publication [6].

The fundamental assumption underlying the PCM is that the state of the dense partonic system can be characterized by a set of one-body distribution functions $F_i(x^\mu, p^\alpha)$. Here i denotes the flavor index ($i = g, u, \bar{u}, d, \bar{d}, \dots$) and x^μ, p^α are coordinates in the eight-dimensional phase space. The partons are assumed to be on their mass shell, except before the first scattering. In the numerical implementation, the continuous parton distribution functions (here we choose the GRV-HO parametrization [7]), are represented by (test) particles

$$F_i(x, \vec{p}) = \sum_{i=1}^N \int d\tau \int dp^0 \epsilon_i \delta(x^\mu - \xi_i^\mu(\tau)) \delta(p^\alpha - q_i^\alpha(\tau)), \quad (1)$$

*on leave from: Variable Energy Cyclotron Centre, 1/AF Bidhan Nagar, Kolkata 700 064, India

where $\xi_i^\mu(\tau)$ and $q_i^\alpha(\tau)$, respectively, denote the space-time position and four-momentum of particle i . τ is a variable (proper time) parameterizing the world-line of a particle. The factor $\epsilon_i = 0, 1$ allows for the creation and annihilation of partons.

Partons generally propagate on-shell and on straight-line paths between scattering events. Before their first collision, partons may have a space-like four-momentum, especially if they are assigned an ‘‘intrinsic’’ transverse momentum.

The time-evolution of the parton distribution is governed by a relativistic Boltzmann equation:

$$p^\mu \frac{\partial}{\partial x^\mu} F_i(x, \vec{p}) = \mathcal{C}_i[F] \quad (2)$$

where the collision term \mathcal{C}_i is a nonlinear functional of the phase-space distribution function. Although the collision term, in principle, includes factors encoding the Bose-Einstein or Fermi-Dirac statistics of the partons, we neglect those effects here.

The collision integrals have the form:

$$\mathcal{C}_i[F] = \frac{(2\pi)^4}{2S_i E_i} \cdot \int \prod_j d\Gamma_j |\mathcal{M}|^2 \delta^4(P_{\text{in}} - P_{\text{out}}) D(F_k(x, \vec{p})) \quad (3)$$

with

$$D(F_k(x, \vec{p})) = \prod_{\text{out}} F_k(x, \vec{p}) - \prod_{\text{in}} F_k(x, \vec{p}) \quad (4)$$

and

$$\prod_j d\Gamma_j = \prod_{\substack{j \neq i \\ \text{in, out}}} \frac{d^3 p_j}{(2\pi)^3 (2p_j^0)} \quad (5)$$

S_i is a statistical factor defined as $S_i = \prod_{j \neq i} K_a^{\text{in}}! K_a^{\text{out}}!$

with $K_a^{\text{in, out}}$ identical partons of species a in the initial or final state of the process, excluding the i th parton.

The matrix elements $|\mathcal{M}|^2$ account for the following processes:

$$\begin{array}{lll} gg \rightarrow gg & gg \rightarrow q\bar{q} & qq \rightarrow qq \\ qq' \rightarrow qq' & qq \rightarrow qq & q\bar{q} \rightarrow q'\bar{q}' \\ q\bar{q} \rightarrow q\bar{q} & q\bar{q} \rightarrow gg & \\ gg \rightarrow q\gamma & q\bar{q} \rightarrow \gamma\gamma & q\bar{q} \rightarrow g\gamma \end{array} \quad (6)$$

with q and q' denoting different quark flavors. The amplitudes for these processes have been calculated in refs. [8, 9] for massless quarks. The corresponding scattering cross sections are expressed in terms of spin- and colour-averaged amplitudes $|\mathcal{M}|^2$:

$$\left(\frac{d\hat{\sigma}}{dQ^2} \right)_{ab \rightarrow cd} = \frac{1}{16\pi\hat{s}^2} \langle |\mathcal{M}|^2 \rangle \quad (7)$$

For the transport calculation we also need the total cross section as a function of \hat{s} which can be obtained from (7):

$$\hat{\sigma}_{ab}(\hat{s}) = \sum_{c,d} \int_{(p_T^{\text{min}})^2}^{\hat{s}} \left(\frac{d\hat{\sigma}}{dQ^2} \right)_{ab \rightarrow cd} dQ^2 \quad (8)$$

The low momentum-transfer cut-off p_T^{min} is needed to regularize the IR-divergence of the pQCD parton-parton cross section. A novel feature of our treatment involves the introduction of a factor $f(x, Q^2)/f(x, Q_0^2)$ for every primary parton involved in a binary collision in expression 8 to account for the difference between the initialisation scale Q_0 and the scattering scale Q . A more detailed description of our implementation is in preparation [6].

One of the most crucial parameters of the PCM is the low momentum transfer cut-off p_T^{min} . Under certain assumptions this parameter can be determined from experimental data for elementary hadron-hadron collisions [10, 11, 12]. In the environment of a heavy-ion collision, colour screening will destroy the association of partons to particular hadrons, since for a sufficiently high density of colour charges, the colour screening radius becomes much smaller than the typical hadronic scale. It is therefore by no means clear whether the p_T^{min} values extracted from hadron-hadron collisions are applicable to heavy-ion collisions. Calculating the colour screening mass μ_D for a set of systems where interactions are governed by specific values of p_T^{min} may allow us to determine a lower boundary for the allowed range of p_T^{min} values, since only values of $p_T^{\text{min}} \geq \mu_D$ are physical.

Following ref. [13], we use perturbative QCD to obtain the time evolution of the screening mass $\mu_D(\tau)$. The parton cascade model provides the phase space distribution of the partons. The general form for the colour screening mass in the one loop approximation is [13, 14, 15]

$$\mu_D^2 = -\frac{3\alpha_s}{\pi^2} \lim_{|\vec{q}| \rightarrow 0} \int d^3 p \frac{|\vec{p}|}{\vec{q} \cdot \vec{p}} \vec{q} \cdot \nabla_{\vec{p}} \left[F_g(\vec{p}) + \frac{1}{6} \sum_q \{F_q(\vec{p}) + F_{\bar{q}}(\vec{p})\} \right], \quad (9)$$

where α_s is the strong coupling constant, the F_i specify the phase space density of gluons, quarks, and anti-quarks and q runs over the flavour of quarks. It is easy to verify that in the case of an ideal gas of massless partons,

where the F_i reduce to Bose-Einstein or Fermi-Dirac distributions (with vanishing baryochemical potential μ_B), Eq. 9 reduces to the standard result for the thermal Debye mass [15, 16]. The partonic distribution will be ini-

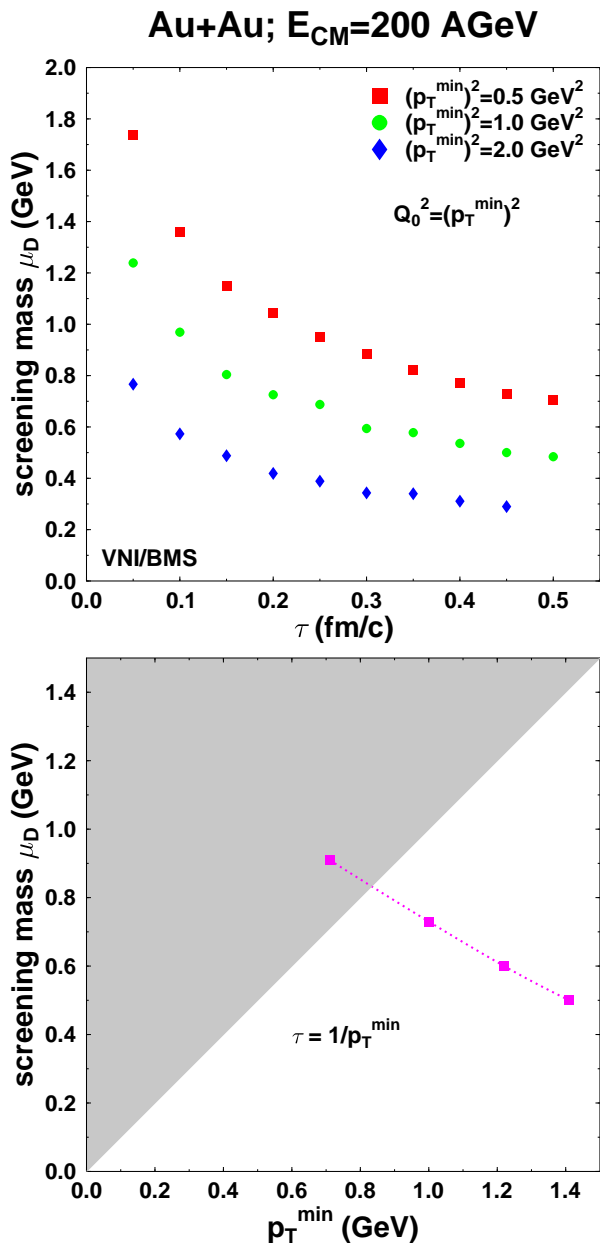


FIG. 1: Top: time-evolution of the screening mass μ_D for several values of p_T^{min} in Au+Au collisions at RHIC. Bottom: μ_D evaluated at $\tau = 1/p_T^{min}$ as a function of p_T^{min} . The gray shaded area symbolizes the unphysical region in which $p_T^{min} \leq \mu_D$ and therefore serves as a boundary for the allowed range of p_T^{min} in Au+Au collisions at RHIC.

tially anisotropic with respect to the beam axis and thus the screening mass of a gluon in the matter may depend on the direction of propagation. We have found that μ_D^\perp differs from μ_D^\parallel by 10% at most and we have therefore assumed $\mu_D = \mu_D^\parallel$ in the following discussion. We also note that the assumptions underlying this method are not strictly applicable to very early times, $\tau < \Delta z$, where Δz is the Lorentz contracted width of the nuclei.

We begin by calculating the screening mass for partonic matter in central Au+Au collisions at RHIC ($\sqrt{s} = 200$ GeV per nucleon pair). The upper frame of figure 1 shows the time evolution of the (transverse) screening mass, calculated according to eq. 9 for several different values of p_T^{min} . The time $t = 0$ marks the maximum overlap of the two colliding nuclei. The time-evolution of μ_D clearly reflects the dynamics of the collision: at early times the density of the system is large, leading to a large value the screening mass μ_D . For later times, density and collision rate (see also figures 2 and 4) decrease, reducing the value of μ_D by more than a factor of two. The strong time-dependence of the screening mass during the early pre-equilibrium phase will have an influence on the equilibration process that is beyond the scope of our present work. A decreasing screening mass implies a rising cross section and thus enhanced multiple rescattering. This aspect is missing in many implementations of the PCM, which assume a time-independent screening mass for the entire duration of the collision [17, 18, 19, 20].

A self-consistent calculation would utilize the time-dependent Debye-mass as the regulator of the interaction among partons instead of introducing a fixed cut-off p_T^{min} as used in our present work. This would be achieved by calculating the parton-parton cross sections in the framework of the hard thermal loop (HTL) approximation [21], which accounts for the full frequency and momentum dependence of the dynamic screening in the high-density, small gradient limit of QCD. The implementation of such a self-consistent dynamical screening mechanism, as formulated recently by Arnold et al. [22] in a PCM remains a major challenge for future work. It should also be noted that, strictly speaking, newly produced partons start providing screening only after $\Delta\tau \sim 1/p_T$ and therefore the concept of a screening mass may not be well justified for times $\tau \leq 1/p_T^{min}$ [14].

In order to determine a lower boundary for the allowed range of p_T^{min} , we calculate μ_D at $\tau = 1/p_T^{min}$ and plot it as a function of p_T^{min} in the bottom frame of figure 1. The gray shaded area symbolizes the region in which $p_T^{min} \leq \mu_D$ and where the procedure to simply cut off the interaction is no longer valid. It therefore serves as a boundary of the allowed range of p_T^{min} for our calculation. We find that the smallest allowed value for p_T^{min} is ≈ 0.8 GeV. The inclusion of higher order radiative corrections and parton fusion processes into our calculation will probably alter this value – we shall study these effects in a forthcoming publication [6].

After having determined the meaningful range of p_T^{min} , our model is applied to the calculation of the time-evolution of the energy-density ϵ generated by hard and semi-hard parton-parton interactions at RHIC: the upper frame of figure 2 shows this time-evolution of ϵ for different values of p_T^{min} , to give an estimate on the sensitivity of ϵ with respect to p_T^{min} . Here, ϵ is calculated via

$$\epsilon(r_T) = \frac{1}{2\pi r_T \tau} \left(\frac{d^2 E_T(r_T)}{dy dr_T} \right)_{y=y_{CM}} \quad (10)$$

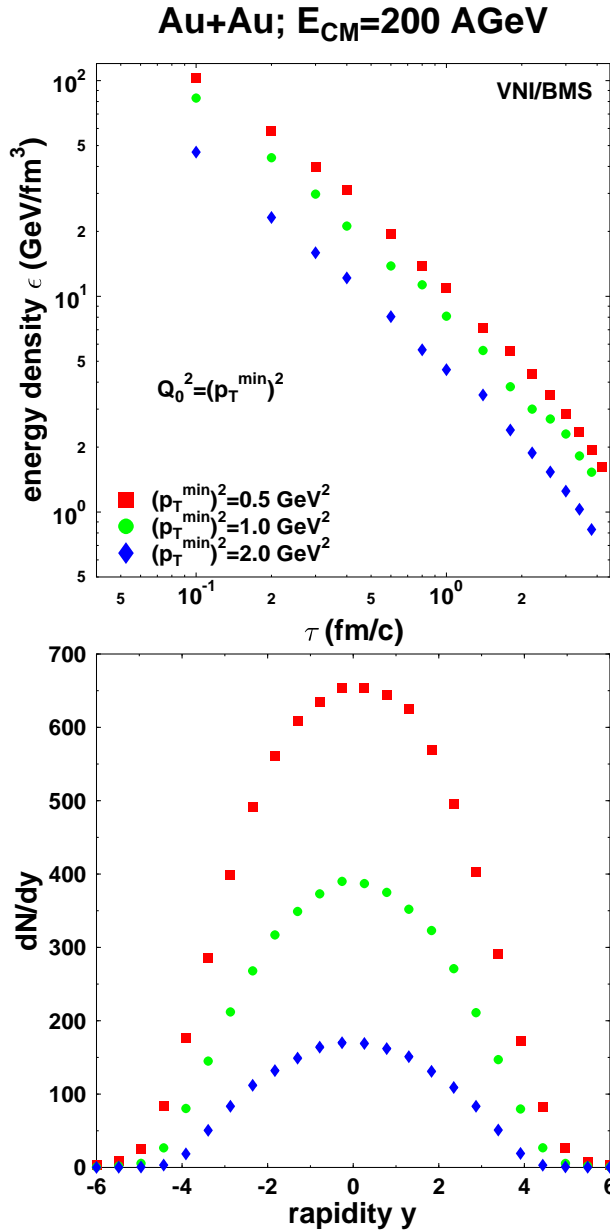


FIG. 2: Top: time-evolution of the energy-density for different values of p_T^{min} . Bottom: rapidity distribution of produced partons generated by hard and semi-hard parton-parton interactions at RHIC.

and

$$\langle \epsilon \rangle = \frac{1}{\pi R_T^2} \int_0^{R_T} \epsilon(r_T) 2\pi r_T dr_T \quad (11)$$

and choosing $R_T = 2$ fm. The maximum energy density obtained in Au+Au collisions in the PCM approach is found to be on the order of 100 GeV/fm³. A detailed analysis shows that for times $\tau \leq 1.0$ fm/c $\epsilon(\tau)$ scales with $1/\tau$ whereas for later times the scaling function is $1/\tau^{4/3}$, most likely signaling a transition from longitu-

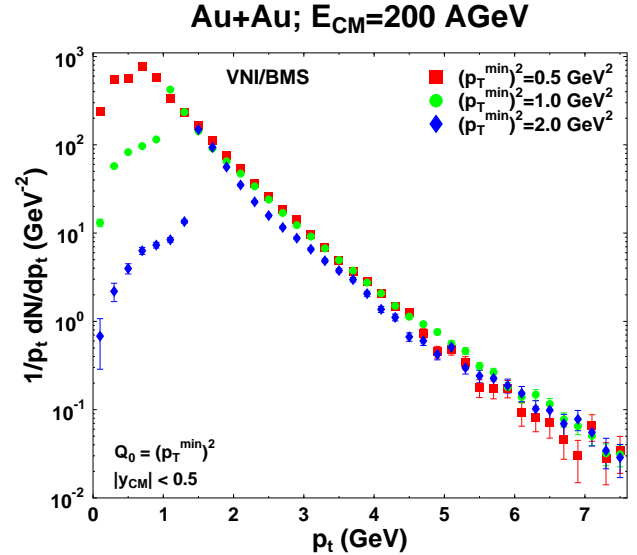


FIG. 3: Transverse momentum spectrum of produced partons in central Au+Au collisions at RHIC for different values of p_T^{min} . Note that the contributions to the spectrum below p_T^{min} stem from parton rescattering.

dinal streaming to a three dimensional expansion. One might be tempted to attribute this scaling to the onset of hydrodynamic expansion. However, the small collision rates at later times (see below) preclude this interpretation.

The bottom frame of figure 2 shows the rapidity distribution dN/dy of produced partons for different values of p_T^{min} . While the distributions cannot be directly compared to experimental data, they provide a lower limit on the entropy produced via hard and semi-hard interactions. Since at hadronization entropy can only be produced or remain constant, the rapidity density of the produced partons provides us with a lower bound for the rapidity density of hadrons compatible with the parameters of our calculation. For $p_T^{min} = 0.7$ GeV the rapidity density of produced partons at mid-rapidity is approximately 650. Assuming parton-hadron duality and entropy conservation during hadronization this number would translate to approximately 430 charged hadrons. In order to be compatible with the data [23], it is important for this number to remain well below the measured value, to allow for additional contributions due to initial and final state radiation as well as soft particle production.

While the absolute values for the energy and rapidity density show a significant dependence on p_T^{min} , the overall shape of the transverse momentum distribution of produced partons changes only in a subtle manner, as can be seen in figure 3. The main impact the choice of p_T^{min} has, is in the low- p_T starting point of the respective distribution – contributions below p_T^{min} stemming from parton rescattering. Naively one would think that

the transverse momentum distribution above the chosen cut-off should not be affected by the choice of the cut-off – however, choosing a low cut-off value increases the amount of parton rescattering which visibly modifies the shape of the p_T spectrum.

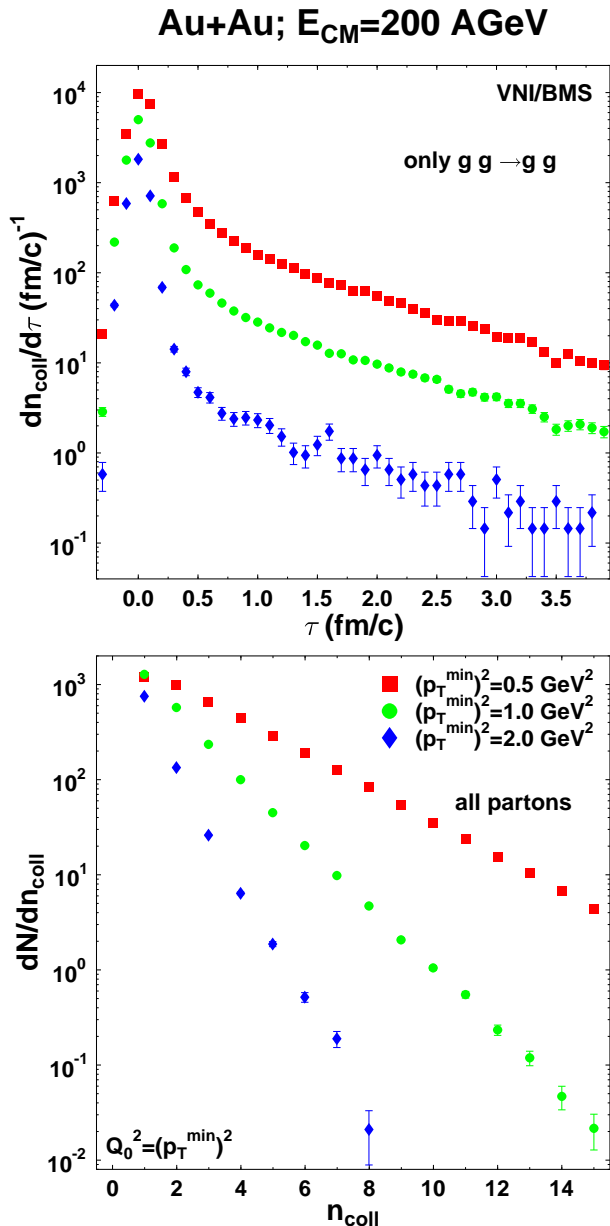


FIG. 4: Top: collision rates for gluon-gluon scattering as a function of time for different values of p_T^{min} . Bottom: parton collision number distribution for different p_T^{min} : the probability for a parton to suffer multiple collisions increases dramatically with decreasing p_T^{min} .

In order to quantify the amount of parton scattering and rescattering we evaluate the collision rates as a function of time and p_T^{min} . The upper frame of figure 4 shows the collision rates for gluon-gluon scattering (glue-gluon collisions account for roughly half the total number of hard scatterings). The time-evolution of the collision rate is clearly peaked at $\tau = 0$ fm/c when the maximum overlap between the two gold nuclei occurs. For $-0.5 \leq \tau \leq 0.5$ fm/c the collision rates show a rough symmetry around $\tau = 0$ fm/c for large values of p_T^{min} , indicating the dominance of primary-primary parton scattering contributions to the collision rate during early times if the cross section is small. This symmetry gets distorted for decreasing p_T^{min} , when secondary parton rescattering increases. For later times the steep decrease in the collision rates flattens out due to parton rescattering, exhibiting a far larger sensitivity on p_T^{min} (and thus the interaction cross section) than at early times. The probability for a parton scattering multiple times can be directly evaluated by plotting the parton collision number distribution, which can be seen in the lower frame of figure 4. While for all cases it is most likely for a parton to only undergo one hard or semi-hard collision, the probability for a parton to suffer multiple collisions increases dramatically with decreasing p_T^{min} .

In a future analysis, we shall attempt to isolate those regions in phase-space in which rescattered partons dominate and identify experimentally accessible observables which are most sensitive to multiple binary perturbative rescattering of partons.

In summary, we have calculated the time-evolution of the Debye-screening mass μ_D for Au+Au collisions at RHIC in the framework of a lowest-order Parton Cascade Model. We have used the screening mass to determine a lower boundary for the allowed range of p_T^{min} values. For that range we determined the energy density reached through hard and semi-hard processes and found that its maximum remains below approx. 70 GeV/fm³. We established a lower bound for the rapidity density of charged hadrons which is compatible with the available data. The possibility of perturbative rescattering among partons has been analyzed and is found to significantly increase with decreasing p_T^{min} .

Acknowledgments

This work was supported by RIKEN, Brookhaven National Laboratory and DOE grants DE-FG02-96ER40945 as well as DE-AC02-98CH10886. One of us (DKS) is especially grateful for the warm and generous hospitality at Duke University, where a large part of this work was done.

[1] A compilation of current RHIC results can be found in: Quark Matter '01, Proceedings of the Fifteenth Interna-

tional Conference on Ultra-Relativistic Nucleus-Nucleus

- Collisions at Stony-Brook, NY, USA, *Nucl. Phys.* **A698** (2002);
 Quark Matter '02, Proceedings of the Sixteenth International Conference on Ultra-Relativistic Nucleus-Nucleus Collisions at Nantes, France, to be published in *Nucl. Phys. A*.
- [2] for reviews on QGP signatures, see
 J. Harris and B. Müller, *Ann. Rev. Nucl. Part. Sci.* **46**, 71 (1996); S.A. Bass, M. Gyulassy, H. Stöcker and W. Greiner, *J. Phys.* **G25**, R1 (1999).
- [3] K. Geiger and B. Müller, *Nucl. Phys. B* **369**, 600 (1992).
- [4] K. Geiger, *Phys. Rept.* **258**, 237 (1995); K. Geiger, *Comput. Phys. Commun.* **104**, 70 (1997).
- [5] L. D. McLerran and R. Venugopalan, *Phys. Rev. D* **49**, 3352 (1994); E. Iancu and L. D. McLerran, *Phys. Lett. B* **510**, 145 (2001); L. McLerran, *Nucl. Phys. A* **699**, 73 (2002).
- [6] S.A. Bass, B. Müller and D.K. Srivastava, manuscript in preparation.
- [7] M. Glück, E. Reya and A. Vogt, *Z. Phys. C* **67**, 433 (1995).
- [8] R. Cutler and D. W. Sivers, *Phys. Rev. D* **17**, 196 (1978).
- [9] B. L. Combridge, J. Kripfganz and J. Ranft, *Phys. Lett. B* **70**, 234 (1977).
- [10] T. Sjostrand and M. van Zijl, *Phys. Rev. D* **36**, 2019 (1987).
- [11] N. Abou-El-Naga, K. Geiger and B. Müller, *J. Phys. G* **18**, 797 (1992).
- [12] K. J. Eskola and H. Honkanen, arXiv:hep-ph/0205048.
- [13] T. S. Biro, B. Müller and X. N. Wang, *Phys. Lett. B* **283**, 171 (1992); H. Satz and D. K. Srivastava, *Phys. Lett. B* **475**, 225 (2000).
- [14] K. J. Eskola, B. Müller and X. N. Wang, *Phys. Lett. B* **374**, 20 (1996).
- [15] O. K. Kalashnikov and V. V. Klimov, *Sov. J. Nucl. Phys.* **31**, 699 (1980) [*Yad. Fiz.* **31**, 1357 (1980)]; V. V. Klimov, *Sov. Phys. JETP* **55**, 199 (1982) [*Zh. Eksp. Teor. Fiz.* **82**, 336 (1982)].
- [16] H. A. Weldon, *Phys. Rev. D* **26**, 2789 (1982).
- [17] B. Zhang, M. Gyulassy and Y. Pang, *Phys. Rev. C* **58**, 1175 (1998); B. Zhang, *Comput. Phys. Commun.* **109**, 193 (1998).
- [18] D. Molnar and M. Gyulassy, *Phys. Rev. C* **62**, 054907 (2000).
- [19] B. Zhang, C. M. Ko, B. A. Li and Z. w. Lin, *Phys. Rev. C* **61**, 067901 (2000).
- [20] Y. Nara, S. E. Vance and P. Csizmadia, *Phys. Lett. B* **531**, 209 (2002).
- [21] E. Braaten and R. D. Pisarski, *Nucl. Phys. B* **337**, 569 (1990).
- [22] P. Arnold, G. D. Moore, and L. G. Yaffe, preprint arXiv:hep-ph/0209353.
- [23] B. B. Back *et al.* [PHOBOS Collaboration], *Phys. Rev. Lett.* **87**, 102303 (2001); B. B. Back *et al.* [PHOBOS Collaboration], *Phys. Rev. C* **65**, 061901 (2002).